APPENDIX

TABLE SI. The energy difference between spin-polarized (along [001] and [100], respectively) and non-spin-polarized as well as energy difference between FM and AFM configurations as a function of Hubbard U.

U (eV)	$E_{[001]}$-E_{NSP} (eV)	$E_{[001]}$-E_{NSP} (eV)	E_{AFM}-E_{FM} (meV)
0.5	-4.439	-4.439	78.165
1.0	-4.984	-4.984	85.989
2.0	-5.897	-5.897	97.992
3.0	-6.603	-6.602	106.546

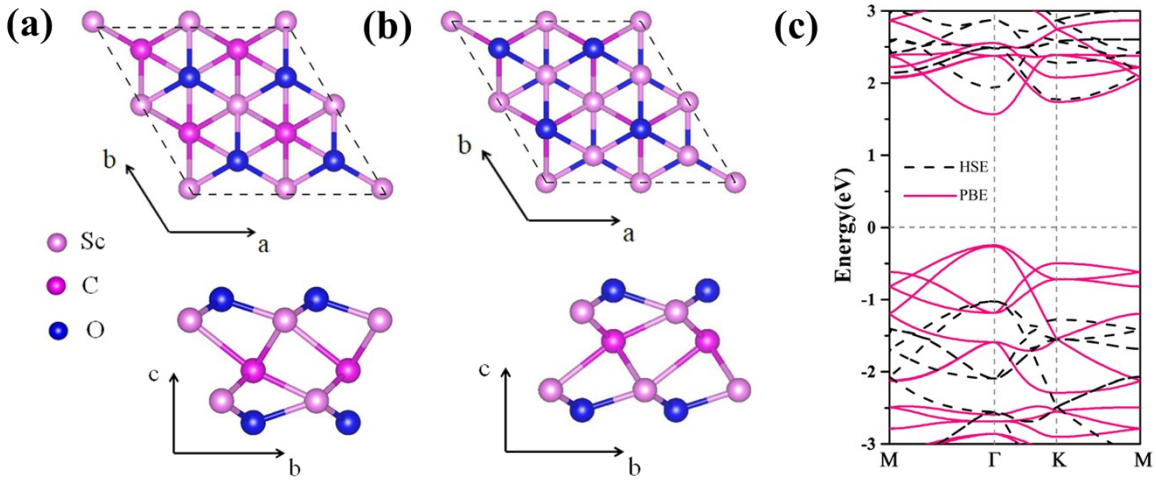

FIG. S1 (a, b) Top and side views of FE ML-Sc_2CO_2. The pink, light purple and dark blue balls represent Sc, C and O atoms, respectively. (c) The energy band structure.

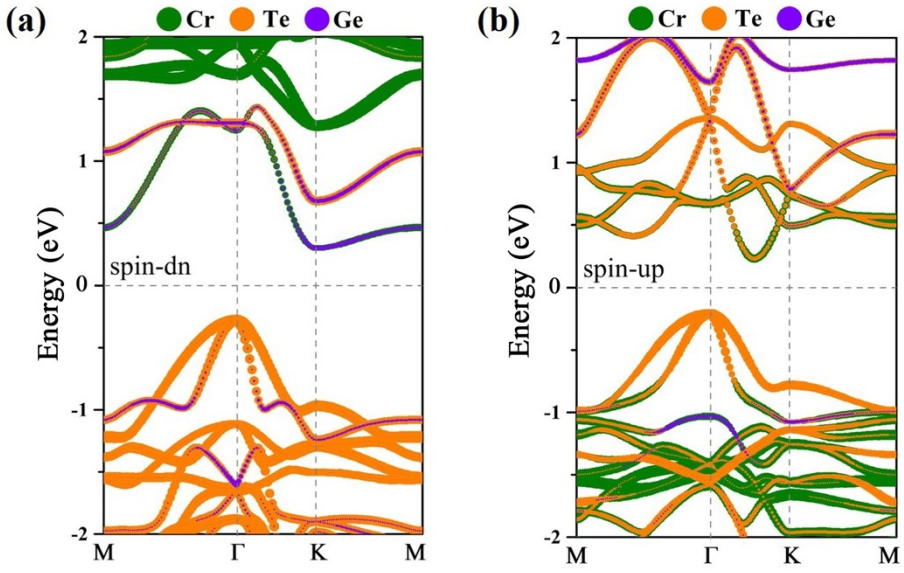

FIG. S2 (a, b) Atomic-resolved band structures of ML-CGT, where the olive, violet and orange symbols denote Cr, Ge, and Te atoms, respectively. The size of the symbols represents the weight of atoms. The Fermi level is set to zero in energy.

TABLE SII. The matrix differences of Cr-*d* between magnetization along *z* and *x* in *Eqs.* (3) and (4).

o^-	o^+

u^-	d_{xy}	d_{yz}	d_{z^2}	d_{xz}	$d_{x^2-y^2}$	d_{xy}	d_{yz}	d_{z^2}	d_{xz}	$d_{x^2-y^2}$
d_{xy}	0	0	0	-1	4	0	0	0	1	-4
d_{yz}	0	0	-3	1	-1	0	0	3	-1	1
d_{z^2}	0	-3	0	0	0	0	3	0	0	0
d_{xz}	-1	1	0	0	0	1	-1	0	0	0
$d_{x^2-y^2}$	4	-1	0	0	0	-4	1	0	0	0

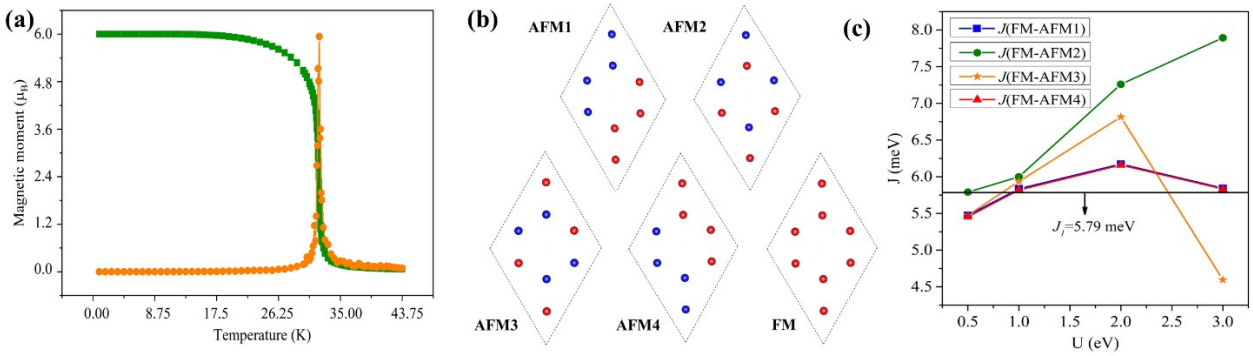

FIG. S3. (a) Temperature-dependent magnetic moment and specific heat for ML-CGT based on MC simulations. (b) Five spin configurations, named AFM1, AFM2, AFM3, AFM4, FM. (c) J under different spin configurations, where J_1 is the nearest exchange interaction when only two configurations are considered.

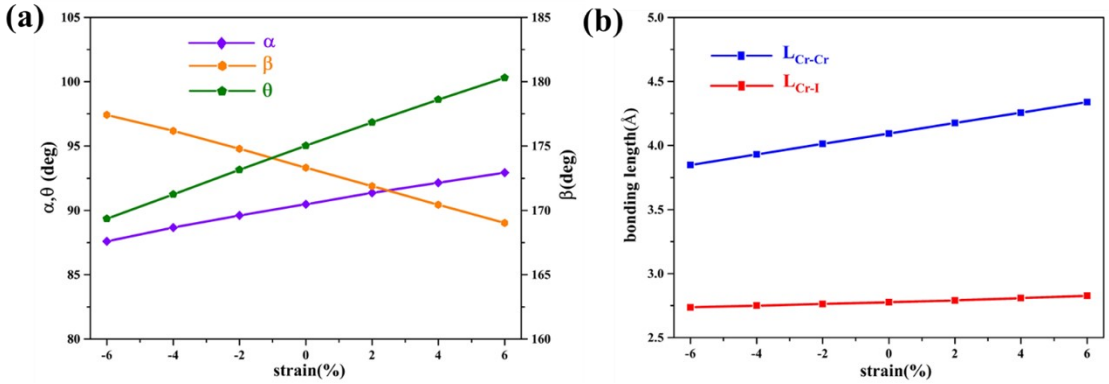

FIG. S4. (a) The bonding angles and (b) Cr-I bonding length (L_{Cr-I}) and Cr-Cr distance (L_{Cr-Cr}) in ML-CrI_3 under compressive (negative sign) and tensile (positive sign) strains, respectively.

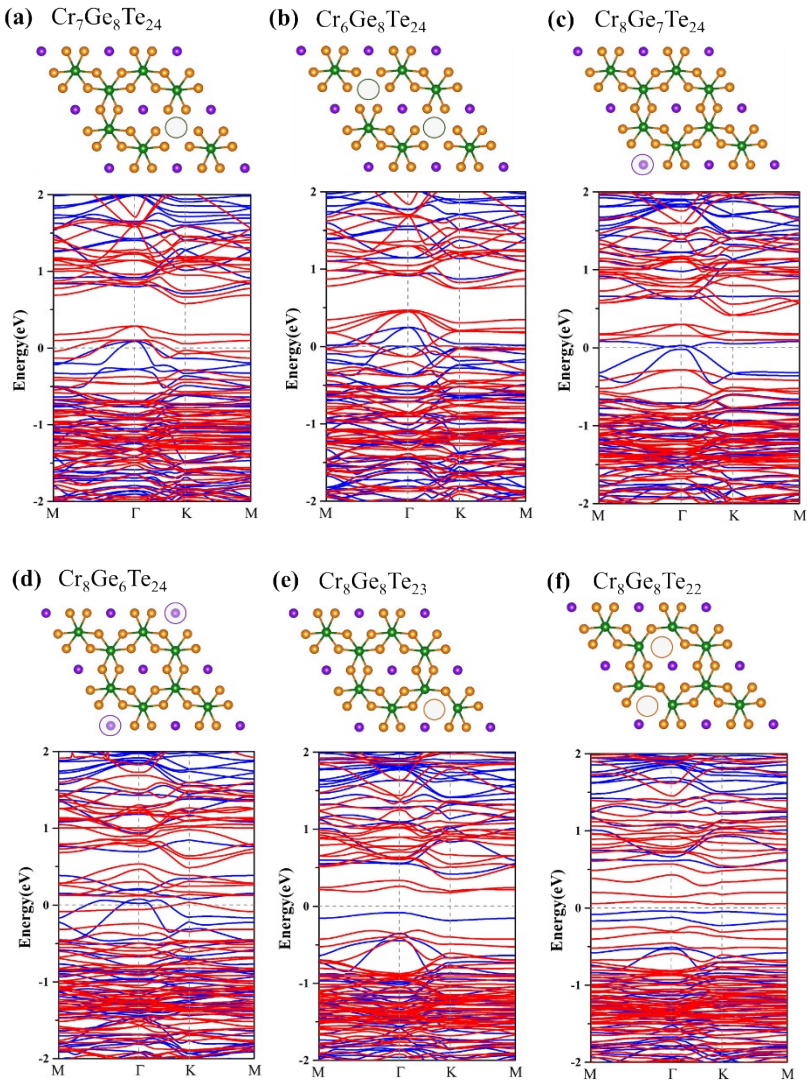

FIG. S5. Three types of defects including Cr, Ge, and Te in ML-CGT and their band structures are shown respectively. The red line represents the energy bands with spin-up, and the blue line represents the energy bands with spin-down. The circles represent the atomic vacancy positions.

TABLE SIII. The formation energy for point defects and change of atomic spin magnetic moments. The formation energy of defects is calculated using the following expression:

$$\Delta E_f = E_V - E_{total} + \sum_{\alpha} n_\alpha \mu_\alpha$$

where E_V and E_{total} are the total energies of ML-CGT with and without atomic vacancies, respectively. μ_α is the absolute value of the chemical potential of atom α, and n_α is the number of such defect atoms; $n_\alpha = -1$ if an atom is added, $n_\alpha = 1$ while if an atom is removed.

$\Delta E_f(eV)$	$m_s^{Cr}(\mu_B/atom)$	$m_s^{Ge}(\mu_B/atom)$	$m_s^{Te}(\mu_B/atom)$

$Cr_7Ge_8Te_{24}$	3.273	3.268	0.024	-0.159
$Cr_6Ge_8Te_{24}$	6.504	3.250	0.023	-0.153
$Cr_8Ge_7Te_{24}$	3.063	3.262	0.033	-0.158
$Cr_8Ge_6Te_{24}$	6.092	3.236	0.033	-0.176
$Cr_8Ge_8Te_{23}$	2.209	3.346	0.014	-0.132
$Cr_8Ge_8Te_{22}$	4.449	3.396	-0.005	-0.141

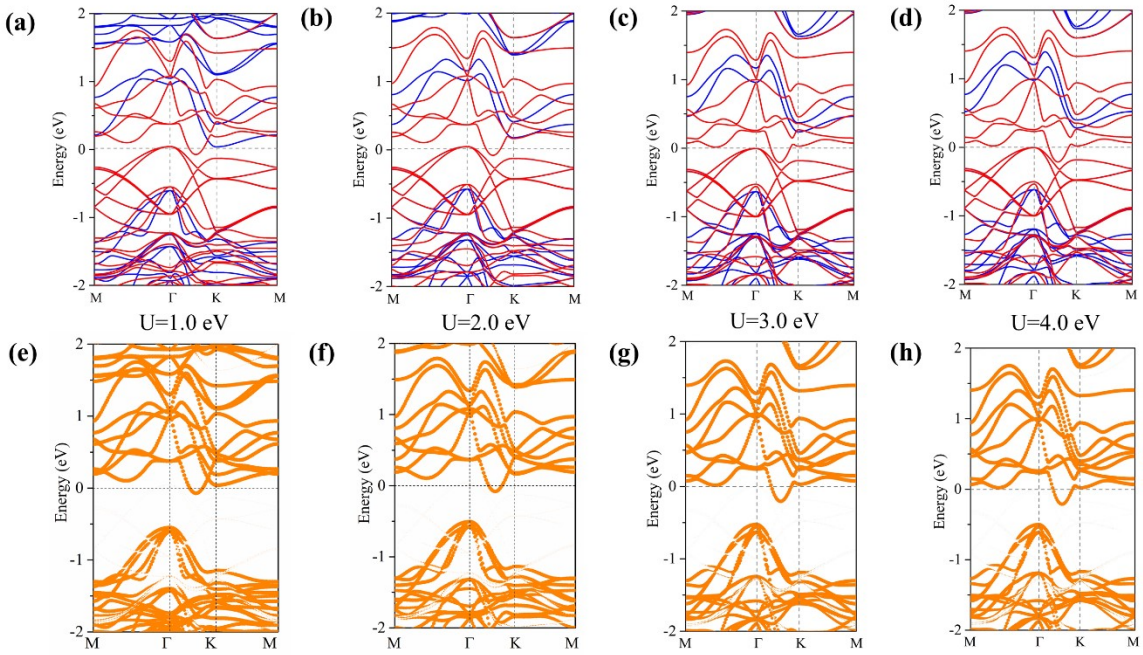

Fig. S6 (a, b, c, d) represent the energy bands of CGT/P↑ at different Hubbard U, where red and blue indicates spin-up and spin-down channels, respectively. (e, f, g, h) represent the energy band components of CGT at different Hubbard U.

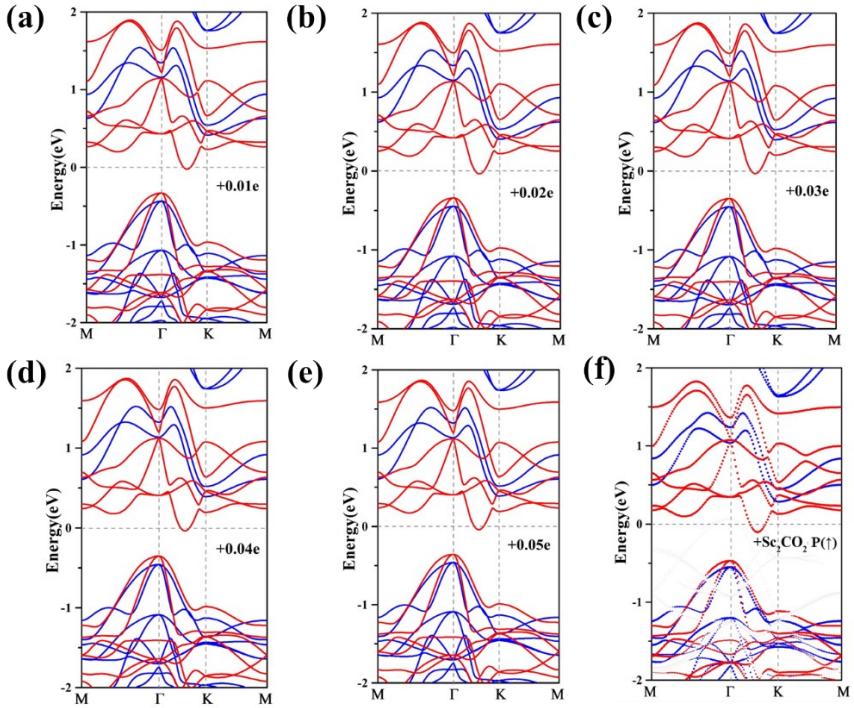

FIG. S7. (a) Band changes after gradually adding electrons to ML-CGT. (b) The energy band structure of CGT/Sc_2CO_2 (P↑). The red line represents the energy bands with spin-up, and the blue line represents the energy bands with spin-down. We can find that the effect of Sc_2CO_2 (P↑) on ML-CGT is equivalent to the injection of electrons.

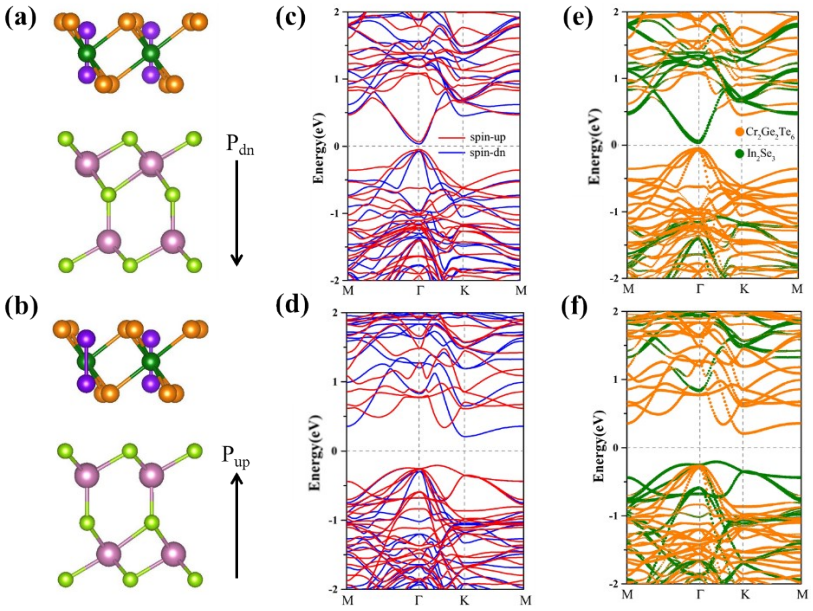

FIG. S8. (a, b) Side views of CGT/In_2Se_3 HTS with FE dipole moment directed upward and downward (P↓ and P↑), respectively, (c, d) The energy band structure of CGT/In_2Se_3. The red line represents the energy bands with spin-up, and the blue line represents the energy bands with spin-down. (e, f) Layer-resolved band structures of CGT/In_2Se_3, where the olive and orange symbols denote In_2Se_3 and CGT, respectively.